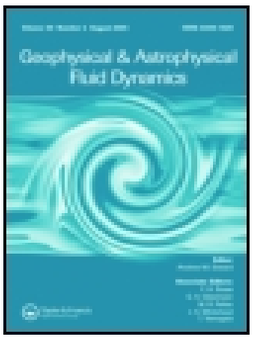

Geophysical & Astrophysical Fluid Dynamics

ISSN: 0309-1929 (Print) 1029-0419 (Online) Journal homepage: www.tandfonline.com/journals/ggaf20

The nonlinear spin-up of a stratified ocean

William K. Dewar, Peter B. Rhines & William R. Young

To cite this article: William K. Dewar, Peter B. Rhines & William R. Young (1984) The nonlinear spin-up of a stratified ocean, Geophysical & Astrophysical Fluid Dynamics, 30:3, 169-197, DOI: 10.1080/03091928408222849

To link to this article: https://doi.org/10.1080/03091928408222849

Published online: 18 Aug 2006.

Geophys. Astrophys. Fluid Dynamics, 1984, Vol. 30, pp. 169–197
0309-1929/84/3003-0169 $18.50/0

Printed in Great Britain

The Nonlinear Spin-Up of a Stratified Ocean

WILLIAM K. DEWAR,† PETER B. RHINES and WILLIAM R. YOUNG‡

The Woods Hole Oceanographic Institution, Woods Hole, MA 02543

(*Received October 11, 1983; in final form June 4, 1984*)

The adjustment of a nonlinear, quasigeostrophic, stratified ocean to an impulsively applied wind stress is investigated under the assumption that barotropic advection of vortex tube length is the most important nonlinearity. The present study complements the steady state theories which have recently appeared, and extends earlier, dissipationless, linear models.

In terms of Sverdrup transport, the equation for baroclinic evolution is a forced advection-diffusion equation. Solutions of this equation subject to a "tilted disk" Ekman divergence are obtained: analytically for the case of no diffusion and numerically otherwise. The similarity between the present equation and that of a forced barotropic fluid with bottom topography is shown.

Barotropic flow, which is assumed to mature instantly, can reverse the tendency for westward propagation, and thus produce regions of closed geostrophic contours. Inside these regions, dissipation, or equivalently the eddy field, plays a central role. We assume that eddy mixing effects a lateral, down-gradient diffusion of potential vorticity; hence, within the closed geostrophic contours, our model approaches a state of uniform potential vorticity. The solutions also extend the steady-state theories, which require weak diffusion, by demonstrating that homogenization occurs for moderately strong diffusion.

The evolution of potential vorticity and the thermocline are examined, and it is shown that the adjustment time of the model is governed by dissipation, rather than baroclinic wave propagation as in linear theories. If dissipation is weak, spin-up of a nonlinear ocean may take several times that predicted by linear models, which agrees with analyses of eddy-resolving general circulation models. The inclusion of a western boundary current may accelerate this process, although dissipation will still play a central role.

†Present address: 12-5 Venable Hall, The University of North Carolina, Chapel Hill, NC 27514.

‡Present address: Scripps Institution of Oceanography, A005, La Jolla, CA 92093.

1. INTRODUCTION

It appears that the Sverdrup balance describes the large-scale north-south transport field, V, of the steady, wind-driven ocean circulation:

$$\beta V = f w_e,$$

where w_e is the Ekman divergence, because of favorable comparisons between observed and predicted transport (Leetma, Niiler and Stommel, 1977). Much of what we feel we know about the circulation of the world ocean has come from applying the above. Still, the Sverdrup balance is not a complete theory of the wind-driven circulation because it makes no statements about the vertical distribution of the transport. A theory which resolves this point has recently appeared (Young and Rhines, 1982; Rhines and Young, 1982 a and b; hereafter RY a and b), the key elements of which are nonlinearity and dissipation. The theory is encouraging as it reproduces several observed features of the North Atlantic, e.g. the northward migration of its deep gyre centers with depth and its basin-scale pools of homogenized potential vorticity (McDowell, Rhines and Keffer, 1982; Holland, Keffer and Rhines, 1983). To develop this theory, RY b solved the statistically steady, quasi-geostrophic equations in the asymptotic limit of vanishingly small eddy viscosity (i.e., large Peclet numbers for potential vorticity diffusion). In the present paper, their calculations are complemented by solving related initial value problems. The solutions will demonstrate the importance of nonlinearity and dissipation in the selection of, and the time scales of approach to, a steady state. We show that asymptopia is reached at rather small Peclet numbers.

In many classical problems, the result of an inviscid spin-up calculation is essentially the same as the steady solution obtained with weak dissipation. Here, however, this is not the case. With realistic forcing amplitudes the problem is nonlinear, the steady inviscid problem is non-unique, and the spin-up, inviscid problem never reaches a steady state.

The equations of motion

Past studies of the wind-driven circulation have employed a variety of approximate equations (e.g. Anderson and Gill, 1975), yet most of

their behavior at the large scales may be deduced from the quasigeostrophic equations. As discussed in RYa, quasigeostrophy accurately describes oceanic evolution on "fast", non-climatic, time scales. We will employ these equations, however it is important to realize that by doing so, we cannot construct a theory which accounts for the basic state stratification; rather we linearize about it, and compute its perturbations due to the large scale wind-driven flow. Quasigeostrophy also requires that we ignore surface thermal structure as the theory is not equipped to handle surfacing isotherms. This is not necessarily a damaging restriction as long as we confine our attention to the wind-driven flow. Pedlosky and Young (1983) and Rhines (1983) have concluded that there are many similarities between wind-driven gyres which are ventilated and those which are not.

Flierl (1978) has shown how the three-dimensional quasigeostrophic equations can be reduced to an infinite, coupled set of two-dimensional equations. Each of those equations predicts the amplitude evolution of a vertical mode, and in total describe quasigeostrophic flow at all spatial scales. For our present purpose it is sufficient, and simplest, to use the two-mode truncation of this infinite set. Equivalently, the dynamics below describe large scale flow in a "two-layer" ocean. This last interpretation will be favoured throughout this article, although it is important to realize that our results, suitably interpreted, apply to an arbitrarily stratified ocean. On large spatial scales the two-layer quasigeostrophic equations are

$$\begin{aligned}
&[\partial/\partial t + f_0^{-1} J(P_1, \cdot)][\beta f_0 y + R_d^{-2}(P_2 - P_1)] = (f_0^2/H_1) w_e - \nabla \cdot \boldsymbol{\Phi}_1, \\
&[\partial/\partial t + f_0^{-1} J(P_2, \cdot)][\beta f_0 y + R_d^{-2}(P_1 - P_2)] = -\nabla \cdot \boldsymbol{\Phi}_2,
\end{aligned} \tag{1}$$

where subscripts denote the layers, $\boldsymbol{\Phi}_i$ the eddy effects in the ith layer.

$$\begin{aligned}
R_d &= (g' H_1)^{1/2}/f_0, \\
g' &= 2g(\rho_2 - \rho_1)/(\rho_1 + \rho_2),
\end{aligned} \tag{2}$$

and P_i the pressure of the ith layer. The remaining terms are catalogued in Table I. We have made the additional, non-essential assumption that the average layer thicknesses are equal; $H_1 = H_2$

TABLE I

Symbol definition

Independent variables	
x, y	horizontal (East, North) coordinates
z	vertical coordinate
t	time
Dependent variables	
α_n	horizontal amplitude functions from the layered model
u_i	ith layer velocity
P_i	ith layer pressure
P	barotropic pressure
Θ	geostrophic contours
ρ	density
ρ_i	ith layer density
q_i	potential vorticity in the ith layer.
Parameters	
f	Coriolis parameter
β	North South gradient of f
H_i	average thickness of ith layer
H	total fluid depth
L	horizontal basin scale
g	gravity
g'	reduced gravity $=\dfrac{2g(\rho-\rho_1)}{(\rho_1+\rho_2)}$
R_d	$\left(\dfrac{g'H_1}{f_0^2}\right)^{1/2}$ = Rossby deformation radius
w_e	Ekman pumping
$\mathbf{\Phi}_i$	Eddy-flux of potential vorticity in the ith layer
μ	Scale of the Ekman pumping
$\delta, \tilde{\delta}$	coefficient of diffusivity
A	bottom drag coefficient
γ	$\dfrac{L_f}{L}$ = non-dimensional radius of forcing

$=\frac{1}{2}H$. The most important simplification made in (1) is the neglect of relative vorticity, which is valid if $U/\beta L^2 \ll 1$.

This neglect "filters" the barotropic mode which translates into a statement that the development of the barotropic Sverdrup transport is instantaneous. This is reasonable physically as the barotropic mode propagates much faster than any baroclinic mode.

2. LINEAR DISSIPATIONLESS OCEAN SPIN-UP

One technique for studying the spin-up of the wind-driven circulation, and the processes responsible for its vertical structure, is to solve an initial value problem. The solution picks out its own final configuration, which of course depends on the physical processes retained in the calculation. This approach has received much attention in the past, and it is enlightening to summarize the results of earlier studies.

Veronis and Stommel (1956) and Anderson and Gill (1975) discussed oceanic spin-up driven by an impulsively applied wind stress. They neglected nonlinearity and emphasized that spin-up was accomplished by baroclinic wave propagation. It was noted by Stommel (1957) that the passage of the wave confined the flow to the upper layer, which may be verified from the appropriate linear solutions of (1). Physically, the lower layer "switches off" because the characteristics for the baroclinic wave, βy, all strike the eastern boundary where there is no mass flux. Westward propagation communicates the no-flux boundary condition to the interior. Note that this process occurs in deep layers *regardless of their number.* On the other hand, the upper layer, which is directly forced, retains its motion, and in the steady state all the transport is confined to the surface layer *no matter how fine it is.*

Anderson and Kilworth (1977) considered the effects of bottom topography. The principle effect of this is to modify the characteristics by altering the fluid depth; however, because of the topography they chose, the interior was still everywhere joined to the eastern boundary by geostrophic contours. While the *initial* barotropic field is altered, the baroclinic wave eventually shuts down the lower layers, and the final state is exactly that of a flat-bottomed ocean.

Continuously stratified fluids fare no better. Charney and Flierl (1981) argued from the density equation that linear, dissipationless equations were consistent only with a motionless interior. Young (1981) amplified these remarks by computing a continuously stratified ocean's linear response to an impulsively applied Ekman pumping. He explicitly showed how the successive arrival of higher order baroclinic modes progressively brings the subsurface fluid to rest. The circulation is eventually confined to a delta-function singularity concentrated at $z=0$ where the forcing is applied.

Although they demonstrate the importance of wave propagation in oceanic adjustment, linear, inviscid, models leave the flow confined to the uppermost layer. When the stratification is continuous this is pathological. We must be suitably cautious in the interpretation of layered model results given the subjectivity with which the depths are assigned to the interfaces. We may of course invoke dissipation, which traps higher modes to the eastern boundary, to inhibit surface "jet" formation. While this softens the delta-function singularity, the solution is still unsatisfactory, for it is sensitive to our viscous parametrization. Further, evaluation of the neglected nonlinear terms shows them to be as large as those retained. Linear, inviscid models simply do not seem to possess the necessary physics to determine an acceptable vertical structure of the wind-driven ocean circulation, so we must investigate the effects of nonlinearity.

3. NONLINEAR OCEANIC SPIN-UP: ANALYTICAL SOLUTIONS

Consider now the two-layer model described by (1), which as remarked earlier is equivalent to a two-mode truncation of the infinite set which describes a continuously stratified fluid (Figure 1). Also, for the moment, consider the fluid to be inviscid, i.e. the eddies to be weak. By adding (1a) and (1b) we obtain an equation for the barotropic mode, $\alpha_0 = P_1 + P_2$, whose solution in terms of w_e is

$$\alpha_0 = -(f_0^2/\beta H_1) \int_x^{x_e} w_e \, dx, \tag{3}$$

where we have satisfied the eastern no-flux boundary condition. Similarly, by subtracting (1a) from (1b), we obtain a simple equation for the baroclinic mode, $\alpha_1 = P_1 - P_2$, which using (3) is

$$(\partial \alpha_1/\partial t) + f_0^{-1} J(\tfrac{1}{2}\Theta, \alpha_1) = \tfrac{1}{2} g' w_e \tag{4}$$

where $\Theta = \alpha_0 + R_d^2 \beta f_0 y$ defines the geostrophic contours. These contours may actually close (see RYb), and thus produce regions which are isolated from the boundaries. This occurs when the barotropic advection of vortex tube length is comparable to β, the planetary

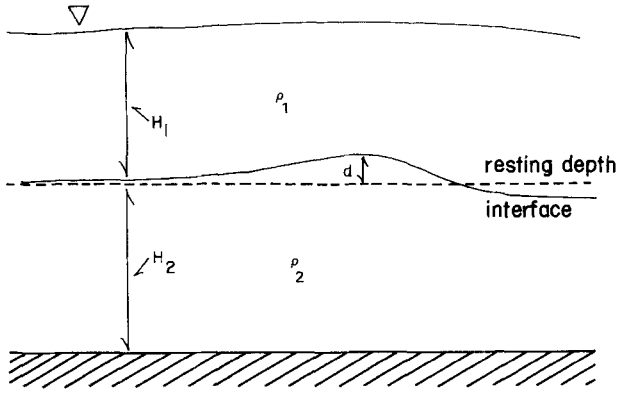

THE TWO LAYER MODEL

FIGURE 1 The dashed line represents the thermocline for the initial resting state. "d" is the deviation of the interface from the dashed line, and is related to the difference of the layer pressures, P_1 and P_2. H_1 and H_2 are the average thicknesses of each layer, and are here assumed equal. ρ_1 and ρ_2 are the layer densities.

potential vorticity. Barotropic flow is then strong enough to reverse the tendency for westward propagation and closed zones ensue.

For example, consider

$$\begin{aligned} w_e &= -2\mu x/L, \qquad \text{if } x^2+y^2 \leqq L_f^2, \\ w_e &= 0, \qquad\qquad \text{otherwise,} \end{aligned} \tag{5}$$

where L is the size of the basin and L_f the radius of the forcing. w_e in (5) is that used in RYb and resembles a titled disk. α_0 becomes

$$\begin{aligned} \alpha_0 &= (f_0^2\mu/\beta H_1 L)(L_f^2 - x^2 - y^2), \qquad \text{if} \quad x^2+y^2 \leqq L_f^2, \\ \alpha_0 &= 0, \qquad\qquad\qquad\qquad\quad \text{if} \quad x^2+y^2 > L_f^2, \end{aligned}$$

and therefore Θ is

$$\begin{aligned} \Theta &= -(f_0^2\mu/\beta H_1 L)\left[x^2+\left(y-\frac{L}{2\sigma}\right)^2 - L_f^2\right], \qquad x^2+y^2 \leqq L_f^2, \\ \Theta &= \beta R_d^2 f_0 y, \qquad\qquad\qquad\qquad\qquad\qquad\quad x^2+y^2 > L_f^2, \end{aligned} \tag{6}$$

where

$$\sigma = f_0 \mu / \beta^2 H_1 R_d^2.$$

The Θ contours inside L_f are arcs of circles centered on $(0, L/2\sigma)$ and, if this point lies within L_f, will close. To insure this, we must have

$$\tfrac{1}{2} < \sigma \frac{L_f}{L},$$

which we shall take for granted. We include a plot of Θ in Figure 2. Note that the closed region is smaller than the forced zone, with the largest closed circle possessing radius $L_f - (L/2\sigma)$, and that outside of L_f, the contours reduce to the zonal contours of the linear problem. The existence of closed geostrophic contours represents the main effect of the nonlinearity.

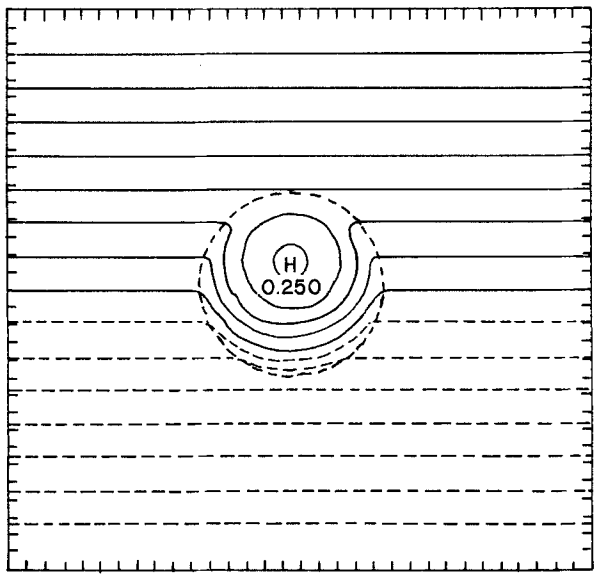

GEOSTROPHIC CONTOURS FOR A NONLINEAR OCEAN

FIGURE 2 The region of forcing, given by Eq. (5), is marked by a dashed line, and is a circle of radius 300 km. The closed geostrophic contours stand out as circles in the center of the diagram.

Inviscid spin-up

Consider the solution to (4). Outside of the closed characteristics, the flow evolves as in all linear problems: the boundary conditions eventually propagate through, shut the lower layer down, and trap the flow to the surface layer. Within the closed contours, however, we obtain quite a different behavior. Transforming to polar coordinates, (r, ϕ), centered on $(0, L/2\sigma)$, (1b) becomes

$$\partial P_2/\partial t - c\,\partial P_2/\partial \phi = 0,$$

where $c = f_0\mu/(\beta H_1 L)$, whose solution is

$$P_2 = \frac{f_0^2\mu}{2\beta H_1 L}\left(L_f^2 - r^2 - r\frac{L}{\sigma}\sin(\phi + ct) - \frac{L^2}{4\sigma^2}\right),$$

which never becomes steady. The initial state within the closed characteristics is remembered indefinitely in the absence of dissipation: the generated baroclinic wave ceaselessly circumnavigates the closed contours. Thus we suspect that in a nonlinear initial value problem, as in the steady theories, eddies are essential to choose a unique solution. Stommel (1957) was the first to remark on the importance of eddy-generated viscosity, specifically lateral Reynold's stress, in stratified circulation theory. We, however, shall assume the principal eddy effect is the vertical transmission of momentum through lateral potential vorticity flux.

The parametrization of eddy effects

Rhines and Holland (1979) have argued that the resultant effect of the eddies on the large scale is the down-gradient transport of potential vorticity. Following them we assume that the proper parametrization of this phenomenon is

$$\nabla \cdot \mathbf{\Phi}_1 = -\tilde{\delta}\nabla^2\alpha_1, \tag{7}$$

i.e. lateral diffusion of potential vorticity.

It is important to note that dissipation is necessary and this parametrization will determine the steady state we obtain. A different

mechanism (e.g. vertical density diffusion) would most likely result in a different final state.

The rate of approach to the steady state will, of course, depend on the strength of the mixing. In any case, dissipation eventually damps the trapped planetary wave, and thus the unsteady solution in the previous section will be impossible. Including dissipation, baroclinic evolution is governed by

$$(\partial\alpha_1/\partial t)+f_0^{-1}J(\tfrac{1}{2}\Theta,\alpha_1)=-\tfrac{1}{2}g'w_e+\tilde{\delta}\nabla^2\alpha_1, \tag{8}$$

which is an advection diffusion equation.

An aside: topographically closed geostrophic contours

At this point it is convenient to interrupt our description of the stratified circulation problem to point out an analogous homogeneous circulation problem.

Equation (8) is similar to that equation governing the circulation of an unstratified fluid over topography

$$\left[\frac{\partial}{\partial t}+f_0^{-1}J(P,\cdot)\right]\left[\beta f_0 y-\frac{f_0^2}{gH}P\right]=-\frac{f_0}{H}J(P,b)+\frac{f_0^2}{H}w_e-A\nabla^2P, \tag{9}$$

where P is the pressure of the fluid and A a bottom drag coefficient (Welander, 1969). The above may be put in the form of (8) if we define

$$\Theta=[\beta f_0 y+(f_0^2 b/H)](gH/f_0^2),$$

and

$$(gH/f_0^2)A=\tilde{\delta},$$

and is then precisely the equation considered by Anderson and Killworth (1975). The primary difference between the homogeneous and stratified problem is that for the homogeneous fluid w_e and b are independent [recall (6)].

Topographic Θ contours can close although this was not considered by Anderson and Killworth. For example, closed regions of f/h are found in the vicinity of the mid-Atlantic Rise. The steady-

state solution to (9) may therefore be found using the same techniques as in RY a, and is given inside the closed zones by

$$\frac{\partial P}{\partial \Theta}=\frac{f_0^2}{AH}\iint w_e dA \Big/ \oint \hat{\mathbf{n}}\cdot\nabla\Theta\, dl. \tag{10}$$

(Young, 1981), where the area integral is over a region bounded by a closed Θ contour, and $\hat{\mathbf{n}}$ is a unit normal of the bounding curve. The flow outside of the closed Θ characteristics is essentially in Sverdrup balance and independent of A. Note that the flow inside the closed regions is $O(1/A)\gg 1$ with respect to the exterior. This is because the interior flow balances wind forcing against dissipation, which requires relatively large interior velocities. A similar balance holds for the baroclinic amplitude in stratified spin-up, showing that even rather weak eddy stresses may efficiently accelerate baroclinic flow within closed contours. The analogy is useful here, but is somewhat limited in scope. The equations lose their resemblance if more than two layers are included. We now return to the stratified spin-up problem.

Lower layer potential vorticity

While (8) is a simple governing equation for baroclinic amplitude, it is convenient to transform it into an equation for the more oceanographically familiar quantity, potential vorticity. This is done using the connection between w_e and Θ,

$$\partial\Theta/\partial x=(f_0^2/\beta H_1)w_e,$$

to eliminate w_e from (8)

$$(\partial q_2/\partial t)+f_0^{-1}J(\tfrac{1}{2}\Theta, q_2)=\tilde{\delta}\nabla^2 q_2, \tag{11}$$

where $q_2=\beta f_0 y+R_d^{-2}\alpha_1$ and is the lower layer potential vorticity from (1). The above equation expresses potential vorticity conservation in the lower layer. The Jacobian term contains both the advection of lower layer vortex stretching by the barotropic flow, the only component of $\mathbf{u}_2$ capable of non-trivial advection of stretching, and the advection of planetary vorticity. The last term represents the dissipation suggested by Rhines and Holland.

In the present model, dynamic evolution is analogous to the advection-diffusion of a passive tracer, thus allowing us to interpret the behavior of this system kinematically. We can thus anticipate some features of the response of the system to the impulsively applied wind stress of (5). The contours of potential vorticity in the lower layer, initially βy, will get wrapped around by α_0, the barotropic flow. Combatting the twisting of the contours is the diffusion of potential vorticity which "reconnects" the geostrophic contours after they are broken at the outermost closed Θ-contour.

4. NONLINEAR OCEANIC SPIN-UP: NUMERICAL SOLUTIONS

Scaling

We consider the given scales to be the basin width "L", the size of the Ekman divergence, μ, and the environmental parameters f_0, β, and H. x and y are scaled by "L" and the barotropic mode by the Sverdrup balance

$$\alpha_0 = (f_0^2 \mu L/\beta H_1)\alpha_0^*,$$

where the * denotes that α_0 is nondimensional. This scaling is also used for the baroclinic mode. The geostrophic contours, Θ, are scaled by βL, and time by $L(\beta R_d^2)^{-1}$, which is the time necessary for a long baroclinic wave to transit the basin, about 400 days. The non-dimensional form of (8) is (dropping *'s)

$$(\partial\alpha_1/\partial t) + J(\tfrac{1}{2}\Theta, \alpha_1) = \delta \nabla^2 \alpha_1 - \tfrac{1}{2} w_e, \tag{12}$$

where

$$\Theta = y + \sigma\alpha_0,$$

and

$$\delta = \tilde{\delta}/(\beta R_d^2 L).$$

The nondimensional form of q_2 is

$$q_2 = y + \sigma\alpha_1.$$

The explicit form of w_e is

$$w_e = -2x,$$

and of α_0

$$\alpha_0 = (\gamma^2 - x^2 - y^2), \qquad \gamma = L_f/L.$$

The condition for closed contours is

$$\sigma\gamma > \tfrac{1}{2}.$$

Using $L = 1000\,\text{km}$, $H_1 = 500\,\text{m}$ (reflecting our interest in the wind-driven gyres above the main thermocline), and typical values for the remaining parameters, $\sigma \sim O(1)$. We have used a value for δ of 0.01. Note that although δ is indeed small, the effective Peclet numbers, based on gyre diffusion and transit times, range from $O(10)$ to $O(1)$, or from conditions where the transit time around the gyre greatly exceeds that necessary for cross-gyre diffusion, to those where the two are comparable. Thus, we consider cases with weak to moderate diffusion.

Equation (12) was solved using a pseudo-spectral technique of the type outlined in Gottlieb and Orszag (1971). With an efficient fast Fourier transform algorithm, the advantage of this method is that the nonlinear terms are evaluated in physical space and transformed to spectral space, thus avoiding costly explicit convolutions. Many other advantages of spectral solutions of partial differential equations have been outlined elsewhere [Orszag and Israeli (1974), Haidvogel (1977), Haidvogel and Rhines (1982)], the most important of which include their rapid convergence (of so-called "infinite order") and zero phase error for resolved waves.

For the present problem, we used a doubly periodic domain, and therefore the double Fourier expansion,

$$\sum_{n=1}^{N_1} \sum_{m=1}^{N_2} a_{mn} e^{-2\pi i np/N_1} e^{-2\pi i mq/N_2} = A_{pq},$$

for all variables. We have also employed a semi-implicit centered

leapfrog time step evaluating the viscous terms at the immediate future and immediate past times to insure stability (Roache, 1977). Integration was initiated using an Euler time step, and the computational mode (Haltiner, 1972) was suppressed by using an Euler time step at every 50th iteration. We used grids corresponding to a physical basins of 2000 km × 2000 km, 2560 km × 2560 km, and 2560 km × 2000 km. Further information about the various runs is given in Table II.

TABLE II

Numerical experiments.

Expt. no.	σ	γ	δ	δx	δy	δt	Basin size	Duration
1	10	0.2	0.05	31.25	31.25	19	2000 × 2000	2.2
2	5	0.3	0.01	31.25	31.25	43	2000 × 2000	2.2
3	5	0.4	0.01	20.00	20.00	19	2560 × 2560	0.5
4	5	0.4	0.01	20.00	31.25	19	2560 × 2000	3.5

The parameters σ, γ, and δ are non-dimensional, δx and δy are in kilometers, δt is in hours, basin size in km, and duration in years.

In Figures 3 and 4, we plot a sequence of diagrams which typify oceanic spin-up. In Figure 3 we catalog baroclinic evolution, and in Figure 4 the time history of potential vorticity. Recall that the displacement of an interface can be related to baroclinic amplitude; hence, Figure 3 contains information about the thermocline. Figures 3a–d and f come from an experiment with $\sigma = 10$ and $\gamma = 0.2$, while Figure 3e is characterized by $\sigma = 0.5$ and $\gamma = 3$. Figure 4 comes from the same experiment as Figure 3e.

The principle features in Figure 3 are the rotation of the thermocline structure within the closed characteristics and the westward propagation of the wave on the open characteristics. The thermocline responds by forming a low pressure center (elevation) in the western half of the forced zone, where the Ekman pumping is directed upward, and a high pressure center to the east. We may think of the advection as moving the western (eastern) columns in the lower layer to the north (south) where they must lengthen (shorten) in order to conserve their potential vorticity. The deformations of the thermocline are not, however, advected by the flow. This is evident in Figure 3b which shows the thermocline one-half revolution after initialization. The structure intensifies as time pro-

gresses (compare Figures 3a and 3d). Were this calculation inviscid, the centers would rotate indefinitely and the amplitude of the pressure extremes would oscillate. Lateral potential vorticity diffusion, however, halts the rotation so that the thermocline asymptotes to states like those in Figures 3d and e. The main structure inside the closed characteristics consists of a linear deepening of the interface from north to south. In Figure 3e this is sufficient to cancel the βy contribution to the lower layer potential vorticity, thus producing a pool of homogenized q. Note that in Figure 3e, the rotation of the thermocline is not quite as pronounced. A perspective plot of the thickness of the upper layer from Figure 3d is contained in Figure 3f and shows that the deepest penetrations of the thermocline occur in the southeastern quadrant and the shallowest in the northwest. The corresponding picture for Figure 3e would look quite similar.

Comparable plan and perspective views of q_2 are shown in Figure 4 [rotation period of 1.2 time units (480 days)]. The βy contribution to the potential vorticity appears as the zonal stripes in the plan views and as the ramp in the perspective plots. The near conservation of q implies that its isolines will be swept around the closed characteristics by Θ. This is implicit in Figure 4b which is roughly one-half rotation period after initiation. Outside of the closed characteristics, fluid simply moves along the geostrophic contours with some slight diffusive modification occurring mostly west and north of the forced zone. As the inner contours are wrapped around, diffusion eats away the structure until the final well-mixed state is achieved. This is reflected in Figure 4h by the plateau in the β-hillside.

It is instructive to comment more fully on the differing results from the two experiments in Figure 3. The primary contrast between them occurs in Figures 3d and e, where we note that the thermocline is oriented in different directions. In Figure 3e, the thermocline is distorted sufficiently so as to homogenize q; a situation which obviously does not occur in Figure 3d. We can understand this result in terms of the Peclet numbers which describe these experiments. The Peclet number, defined as $r^2\sigma/2\pi\delta$ (essentially gyre diffusion time divided by circulation time), where r is the radius of the largest closed geostrophic contour, is 0.75 for Figures 3a–d ($\gamma=0.2$) and 3.2 for Figure 3e ($\gamma=0.3$). Thus the $\gamma=0.2$ experiment is more diffusive than the $\gamma=0.3$ experiment, which homogenizes. The

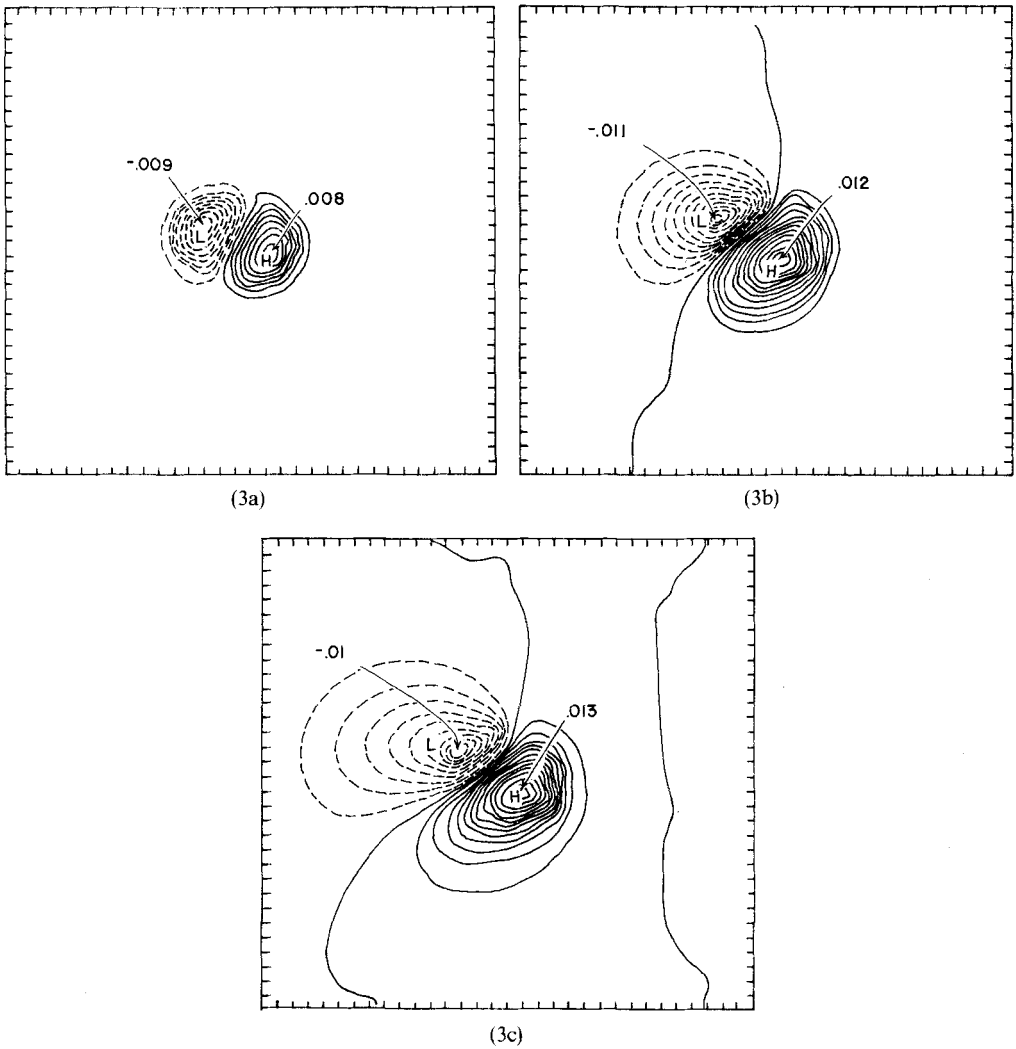

FIGURE 3 Figures 3a–3e represent a typical sequence for an adjusting thermocline. Figures 3a–d are from an experiment with $\sigma = 10$ and $\gamma = 0.2$. The disk of non-zero forcing is of radius 200 km. A time unit corresponds to 400 days and one rotation period of the closed characteristics is 240 days. The diffusivity parameter δ is 0.05, and the plots are at times 40 days (a), 160 days (b), 320 days (c), and 480 days (d). Figure 3e is from an experiment with $\sigma = 5$ (rotation period of 480 days), and $\gamma = 0.3$

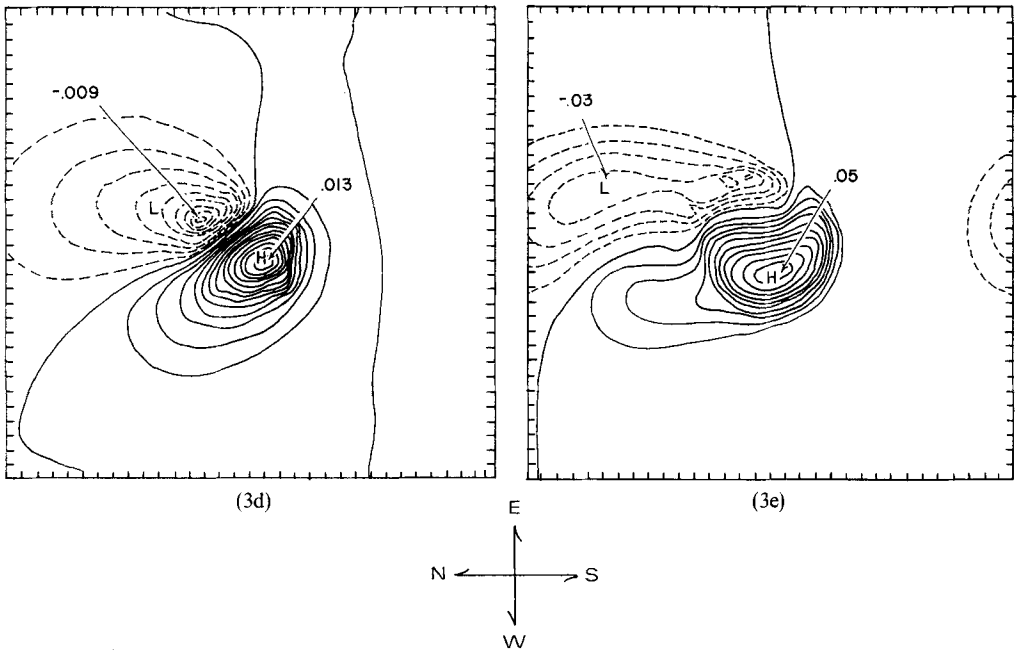

(3d) (3e)

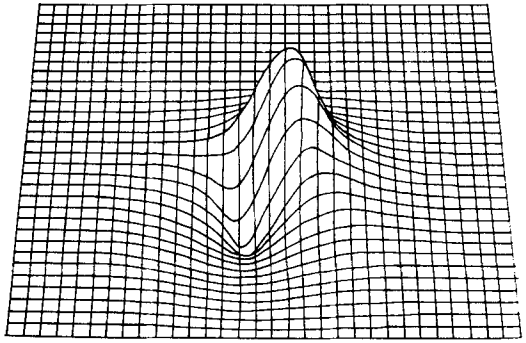

(3f)

THE EVOLUTION OF THE THERMOCLINE

($L_f = 300$ km), and corresponds to a time of 600 days. Finally, we present in "f" a perspective view of the upper layer thickness from the experiment of Figure 3a–d. (f) corresponds to (c), a time of 320 days. The perspective is that of a viewer looking towards the east at, and slightly down on, the interface. The Peclet number of Figure 3a–d is 0.75, while that of Figure 3e is 3.2.

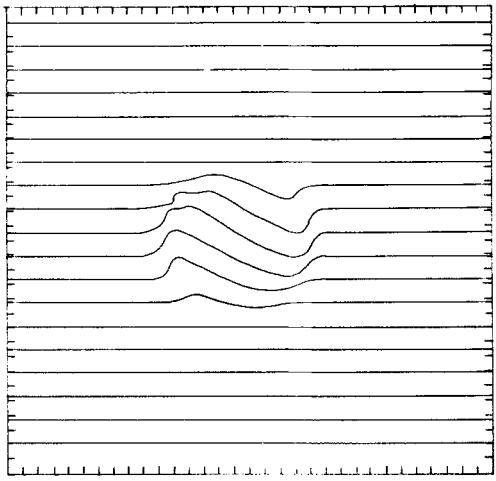

(4a)

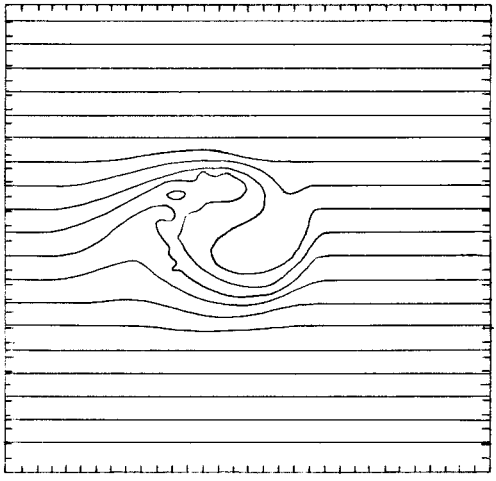

(4b)

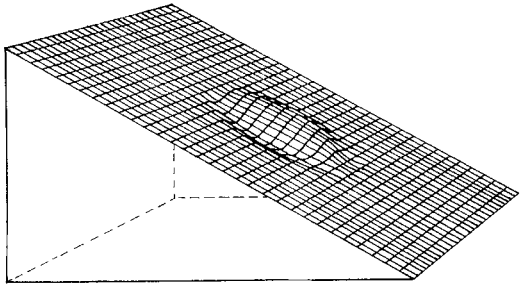

(4e)

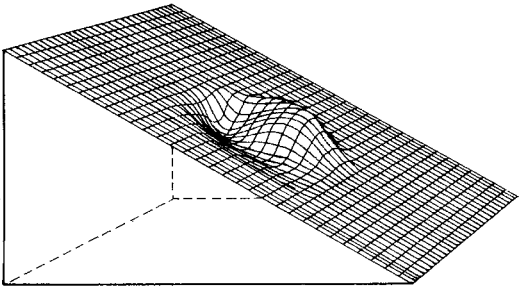

(4f)

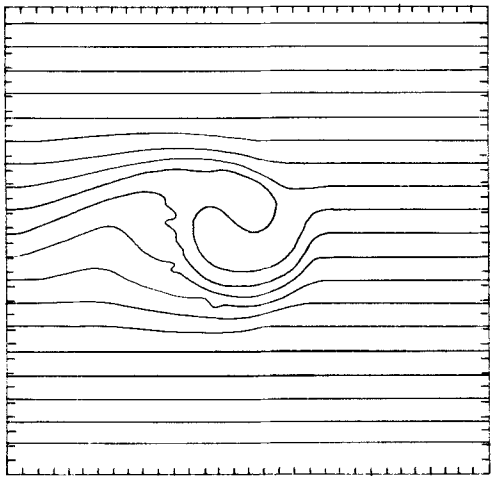

(4c)

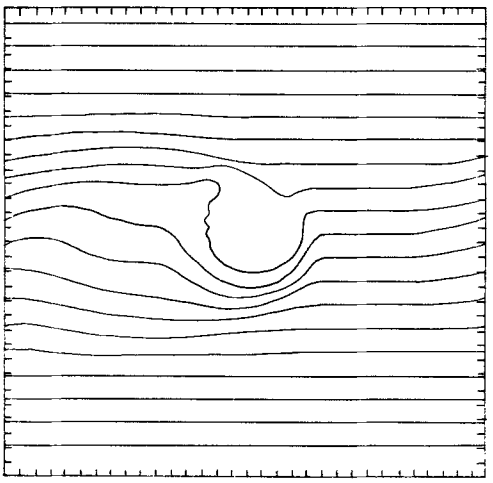

(4d)

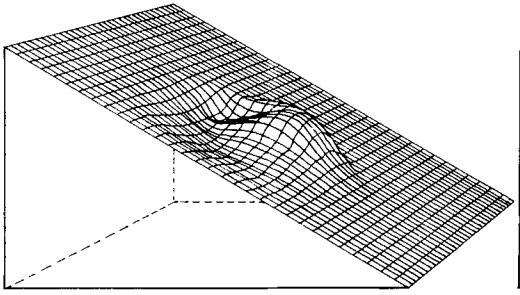

(4g)

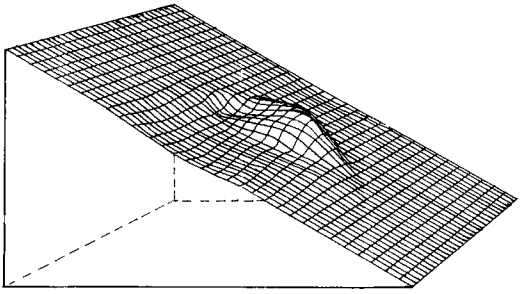

(4h)

THE POTENTIAL VORTICITY OF THE LOWER LAYER

FIGURE 4 $\sigma = 5$, and $\gamma = 0.3$ (or a rotation period of 480 days and a forced zone of radius 300 km). The plots are from times 40 days, (a), 240 days (b), 360 days (c), and 520 days (d). Directly under them in "e" through "h" are perspective views of the same information. The perspective is that of a viewer looking slightly down on the $z = 0$ plane from the south-west toward the north-east.

stronger the diffusion, the more effect the external βy potential vorticity has on the interior steady-state q, until homogenization becomes impossible. It is interesting that q is homogenized in the $\gamma = 0.3$ experiment (Peclet number = 3.2). Here diffusion is moderate and yet, for this particular, simple streamline pattern, homogenization still occurs. Obviously, the drive for homogenization is powerful, holding down to Peclet numbers of order one.

Continuing with Figure 4, the disturbance outside of the closed contours propagates as a nondispersive planetary wave at a speed of βR_d^2. After 520 days (Figures 4d and 4h), it has traversed a little more than one non-dimensional spatial unit, or dimensionally 1000 km. Note also that the q appears to exit the closed zone in the northwestern quadrant, where there is an effective stagnation point. This point is located at the spot where eastward barotropic advection exactly matches westward β propagation; it is at this point in our fixed frame that the Θ velocity identically vanishes. Potential vorticity is actually diffusing out of the closed zone all along the limiting contour. We notice it in the northwestern quadrant because the external flow sweeps first south and west and then north and west around the closed zone, and concentrates the diffused potential vorticity near the stagnation point.

These figures show that with nonlinearity and dissipation we obtain a solution which approaches a steady state. Although the final state depends on the down-gradient mixing of q, the well mixed potential vorticity pool arrives at a value determined by the exterior q field and is therefore *independent of the actual value of the dissipation coefficient*. These features of the current model were lacking in the linear and/or inviscid models mentioned earlier.

One of the important implications of these experiments concerns the time scale, τ, of oceanic spin up. The τ's suggested by the linear initial value problems mentioned earlier depended essentially on the transit time of baroclinic waves, which in the present experiments corresponds to a non-dimensional time span of 1 (400 days). In Figure 5, we show q plots from an experiment in which it is quite evident that the ocean is still in a period of transition after two non-dimensional time units have elapsed. While baroclinic propagation is obviously a major feature of the time-dependent solution, other effects are responsible for the transition to a steady state.

Recalling that the area inside the closed regions is in solid body rotation, the last few plots of Figure 5 demonstrate that the eddy

flux of q is the important process in the approach to steady state of the present model. It is clear that the q inside the gyre is being eaten away by diffusion, so that by time 2.4 we are no longer able to distinguish any structure. This numerically computed spin-up time is in excellent agreement with that time necessary for diffusion to penetrate a distance r to the center of the closed zone

$$T_d = r^2/4\delta.$$

The nondimensional radius of the closed Θ region in Figure 5 is (0.3), and $\delta = 0.01$; thus, $T_d = 2.25$. Similar agreement was found for all the experiments listed in Table II.

Possible effects of shear

The barotropic advection field in these experiments is in some ways rather special. The Ekman pumping produces a barotropic flow which rotates uniformly, and is unable to augment the dispersal of q as would occur if the flow had a non-trivial shear (Taylor, 1953). It is therefore useful to determine how the effects of shear might influence our results.

We show in Figure 6 an experiment on the advection and diffusion of a passive tracer in a sheared velocity field. The evolution of the tracer patch is governed by (11). The primary difference between this experiment and the previous ones is that the initial distribution for the tracer is a Gaussian, which differs from the initial planetary distribution of potential vorticity, βy. Otherwise, this experiment is useful for demonstrating how more complicated or realistic wind stress distributions might affect spin-up. The stream function, Θ, in Figure 6 is given by

$$\begin{aligned} \Theta &= [x^2 + (y + \tfrac{1}{2}\sigma)^2] - \frac{1}{4\sigma^2}, \qquad r < 1, \\ \Theta &= [2 - e^{-(r-1)}] + y/\sigma, \qquad r > 1. \end{aligned} \tag{13}$$

and possesses closed characteristics (see Figure 6a). The center of the closed area is in solid body rotation; however, as we move towards its flanks, the velocity field develops strong shear.

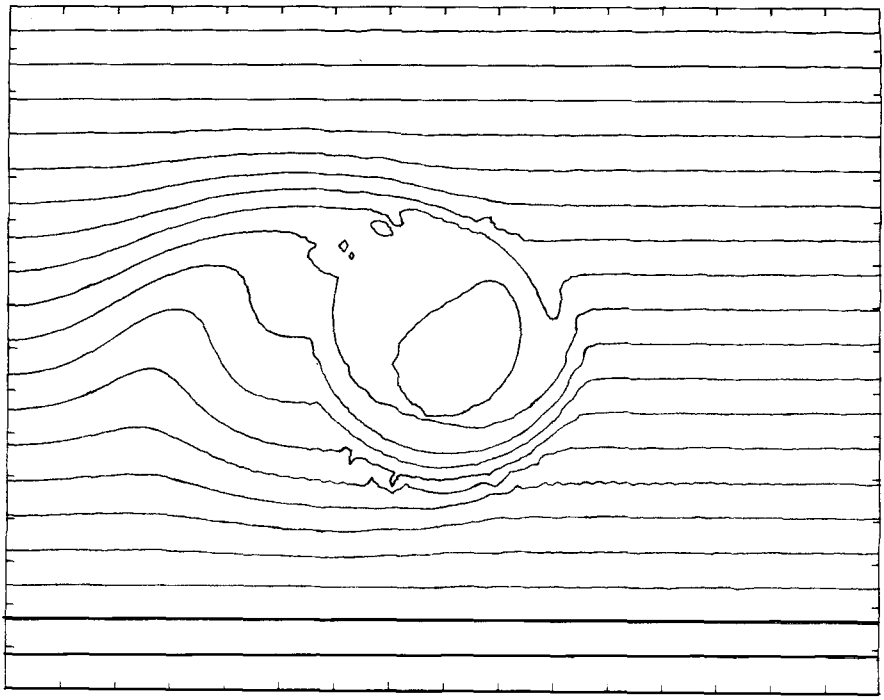

(5a)

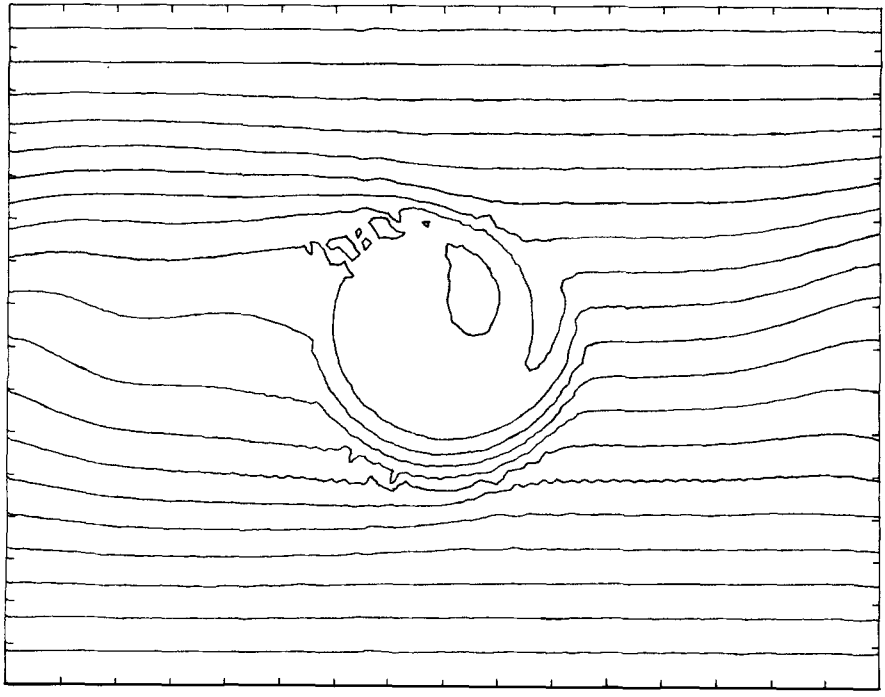

(5b)

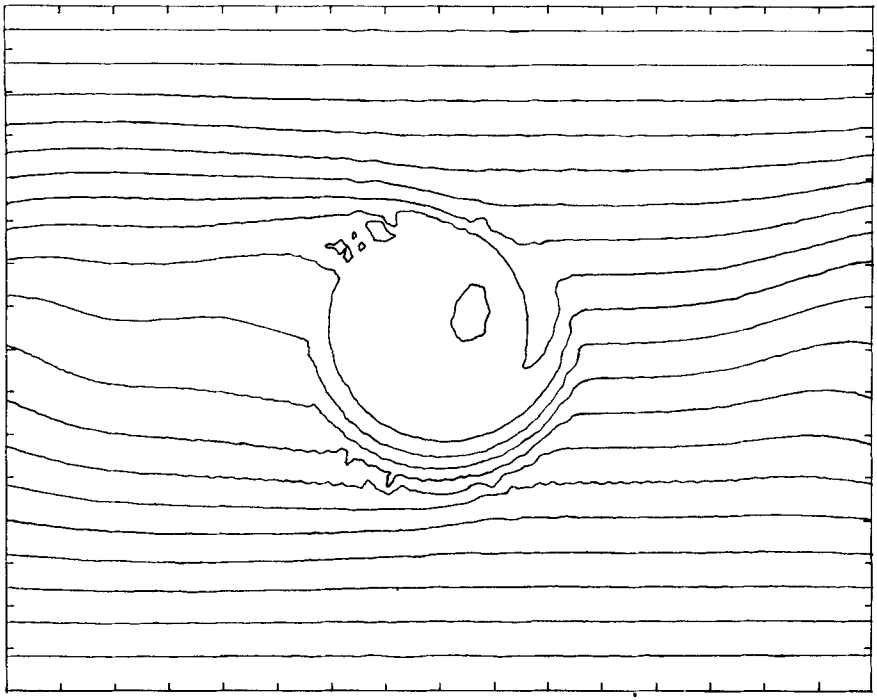

(5c)

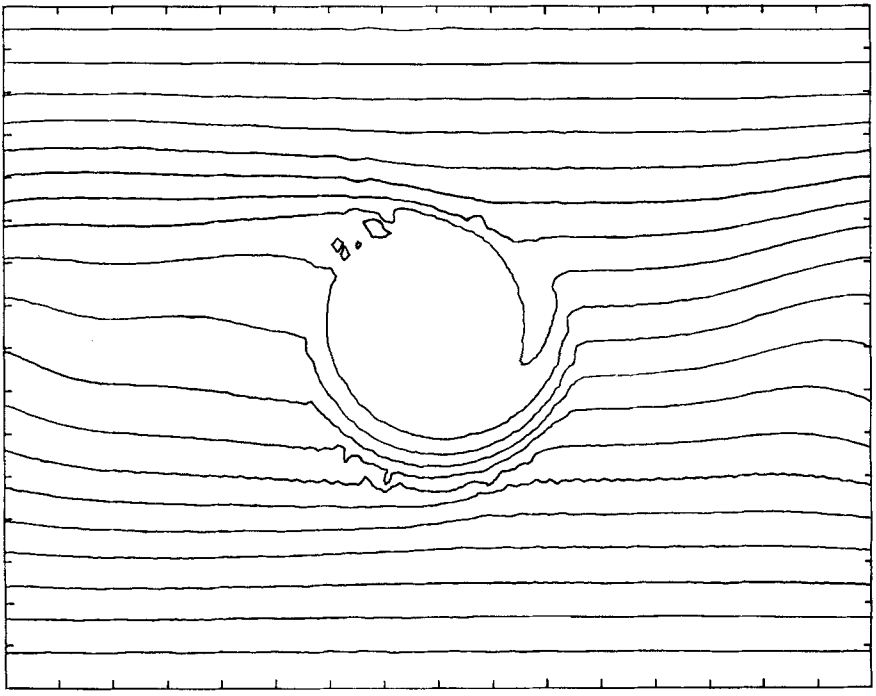

(5d)

THE TIME-SCALE OF ADJUSTMENT

FIGURE 5 $\sigma = 5$ and $\gamma = 0.4$ (rotation period 480 days and radius of forced zone of 400 km). "a" corresponds to 480 days, "b" to 880 days, "c" to 920 days, and "d" to 960 days. With respect to the resolution of these diagrams (contour interval = 0.02) all structure is lost at time $t = 960$ days which agrees well with the diffusive time scale of 900 days. The Peclet number here equals 9.

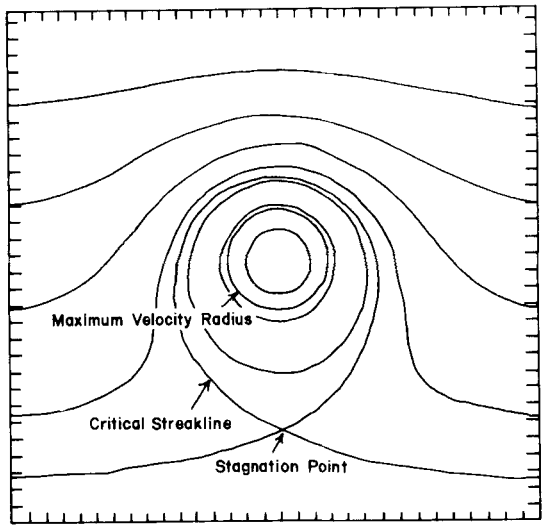
Maximum Velocity Radius
Critical Streakline
Stagnation Point

(a)

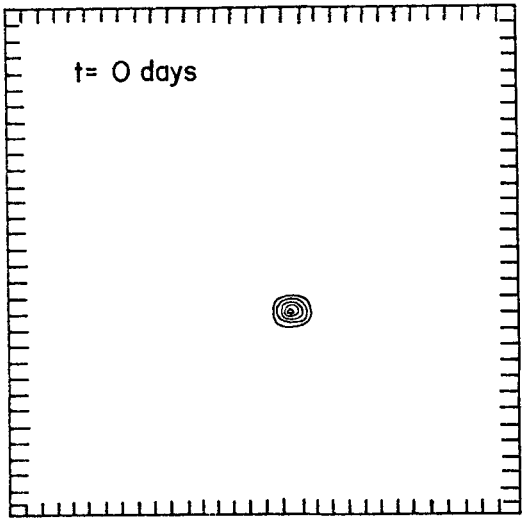
t= 0 days

(b)

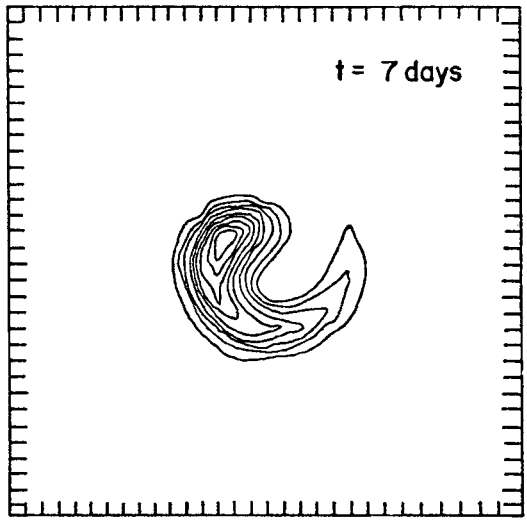

(c)

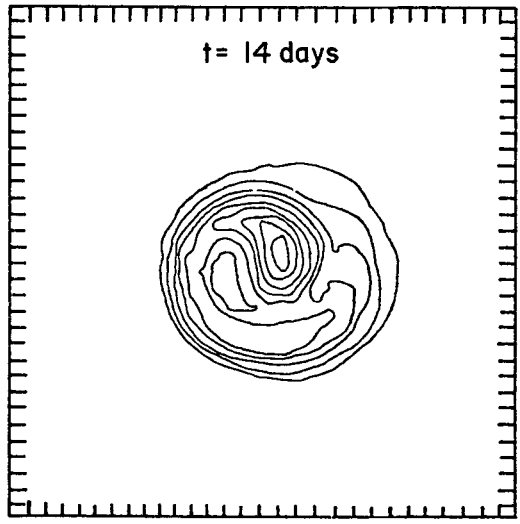

(d)

THE EFFECT OF SHEAR ON PASSIVE SCALAR DIFFUSION

FIGURE 6 The governing equation was (12) with $\delta = 0.04$, $w_e = 0$, and the advection field Θ as shown in "a". The initial condition for the scalar was chosen to be a delta function located within but near the edge of the trapped zone. The evolution of the scalar is shown in "b" through "d". The circulation time of the trapped zone is 2 days.

The dispersant is rapidly homogenized on those streamlines near the edge, i.e. where the flow is strongly sheared. Indeed, this spread along streamlines turns out to be the primary effect of shear-augmented dispersion. Diffusion causes the material to spread across the streamlines, and then differential velocity accelerates its transport along them. Because these streamlines are closed, the marked fluid returns to its initial point with the tracer having been wrapped around the contours in the process. Isolated bits of tracer are "averaged" around the streamlines in this manner. Rhines and Young (1983) have argued that the time scale of this smoothing for gyres without western boundary currents is given by:

$$T_a = \left(\frac{L_f}{U}\right)\left(\frac{UL_f}{\delta}\right)^{1/3},$$

which in our case is substantially faster than diffusion time.

The initial condition $q = \beta y$, when combined with a north-south symmetric advection field such as we are using, is in some ways doubly special. The "average" q on any streamline is independent of the streamline; thus, when shear dispersion is in operation the homogenization of the entire closed region will occur, almost by default, in an averaging time. This also characterizes the experiments of Weiss (1966) and Moffatt and Kamkar (1983). It is doubtful however that the ocean is characterized by this rather special configuration, with a wind field and ambient potential vorticity related such that the average q over any geostrophic contour is the same. If this special relationship is broken, the shear-dispersion averaging process, which will still operate, will not entirely homogenize the region, but only average the q around streamlines.

An example of this is given in Figure 6. We still see structure in the tracer field towards the end of the experiment. At the flanks of the trapped zone, very little of that structure occurs along the streamlines. In that state, shear dispersion is disabled. Further evolution of tracer field, including its eventual homogenization across the streamlines, will occur by diffusion. Thus gyres without boundary currents have a rapid adjustment phase, intermediate between the diffusion time and the advection time, and then a slow phase of mixing across streamlines, requiring a diffusion time. Estimates (Young, 1983) suggest that boundary currents can act as a "mixing valves" and homogenize tracers much more rapidly.

5. SUMMARY

In the present paper, we have studied a nonlinear model of the spin-up from rest of a stratified ocean subjected to an impulsively applied wind stress. The unnatural constraint on the wind that it input no net potential vorticity at any latitude removes the need for western boundary layers.

The essential ingredients in the present model are the nonlinear interactions of the barotropic and baroclinic modes and the dissipation. Nonlinearity, equivalent to barotropic advection of vortex tube length, affects the ambient potential vorticity of the lower layer. For realistic wind strengths, this effect can overcome the tendency for westward propagation due to planetary vorticity and produce regions of closed geostrophic contours. Since the characteristics, or paths of wave propagation, for these regions do not strike lateral boundaries, the no-flux conditions there do not determine the lower layer flow. Rather, as the flow evolves, the baroclinic wave is trapped within these contours and diffusion becomes essential for the production of a steady state. Our particular choice for dissipation assumes that the eddies effect a lateral diffusion of potential vorticity, hence, our solutions approach the state of uniform q predicted elsewhere (RYa). We have also shown that homogenization occurs well into the range of moderate dissipation. We stress that a different dissipative mechanism would lead to different results.

Finally, the time scale for spin-up was shown to depend on dissipation. This view differs from that suggested in linear models, where the transit time for the baroclinic wave was the lapse necessary for the ocean to adjust. Dissipation, or the eddy field, is generally considered weak; therefore, spin-up time should exceed that necessary for baroclinic wave propagation. Holland (1982), using eddy resolving circulation models, has found spin-up times of roughly 10 years. The present model, using somewhat smaller basins, requires anywhere from 1 to 4 years. We have also discussed the implications of our uniformly rotating advection field and have argued using numerical examples that the inclusion of shear dispersion does not alter the basic results of this paper. The fundamental difference between our results and those in the most general problem is that the intermediate stage of spin-up is characterized by a rapid adjustment to a state of homogenous q on streamlines. Once the

potential vorticity is pinned to the streamlines, the homogenization of q across streamlines proceeds only by diffusion, unless, of course, the initial q distribution is uniform when averaged about streamlines, or boundary layers are present.

Acknowledgements

The authors wish to thank Drs. John M. Bane, Glenn R. Flierl, and Dale B. Haidvogel for a number of helpful discussions. Support for this research was provided by NSF Grant OCE 80-23763. This manuscript was prepared at the University of North Carolina where one of us (WKD) was supported by ONR Grant No. N00014-77-C-0354. WRY has been supported at the Scripps Institution of Oceanography through ONR Grant N00014-79-C-0472. Credit for the careful editing of this paper must go to Ms. Diane Hamm and Schatzie Fisher. This is contribution number 5421 from the Woods Hole Oceanographic Institution. Contribution of the Scripps Institution of Oceanography, new series.

References

Anderson, D. L. T. and Gill, A. E., "Spin-up of a stratified ocean with applications to upwelling," *Deep-Sea Res.* **22,** 583–596 (1975).

Anderson, D. L. T. and Killworth, P. D., "Spin-up of a stratified ocean, with topography," *Deep-Sea Res.*, **24,** 709–732 (1975).

Charney, J. G. and Flierl, G. R., "Oceanic analogues of large-scale atmospheric motions," *Evolution of Physical Oceanography: Scientific Surveys in Honor of Henry Stommel*, B. A. Warren and C. I. Wunsch, Ed., MIT Press, Cambridge, Massachusetts and London, England (1981).

Flierl, G. R., "Models of vertical structure and the calibration of two-layer models," *Dynam. Atmos. Oceans* **2,** 341–381 (1978).

Gottlieb, D. and Orszag, S. A., "Numerical analysis of spectral methods: theory and applications," *CBMS-NSF Monograph Number 26*, Society for Industrial and Applied Mathematics, Philadelphia (1977).

Haidvogel, D. B. "Quasigeostrophic regional and general circulation modelling: An efficient pseudospectral approximation technique," *Computing Methods in Geophysical Mechanics* **25,** American Society of Mechanical Engineers, New York (1977).

Haidvogel, D. B.. and Rhines, P. B., "Waves and circulation driven by oscillatory winds in an idealized ocean basin," *Geophys. Astrophys. Fluid Dynam.* **25,** 1–63 (1984).

Haltiner, G. J., *Numerical Weather Prediction*, Wiley, 317 pp. (1971).

Holland, W. R., "Regions of uniform potential vorticity in an ocean circulation model with mesoscale resolution," In preparation (1982).

Holland, W. R., Keffer, T. and Rhines, P. B., "The dynamics of the oceanic general circulation: the potential vorticity field," *Nature*, In press (1984).

Leetma, A., Niiler, P. and Stommel, H., "Does the Sverdrup relation account for the mid-Atlantic circulation?" *J. Mar. Res.* **35,** 1–10 (1977).

McDowell, S. P., Rhines, P. B. and Keffer, T., "North Atlantic potential vorticity and its relation to the general circulation," *J. Phys. Oceanogr.* **12,** 1417–1436 (1982).

Moffatt, H. K. and Kamkar, H., "The time-scale associated with flux expulsion," pp. 91–97 in *Stellar and Planetary Magnetism*, A. M. Soward, ed., Gordon and Breach, New York, London, Paris (1983).

Orszag, S. A. and Israeli, M., "Numerical simulation of viscous incompressible flow," *Ann. Rev. Fluid Mech.* 218–318 (1974).

Pedlosky, J. and Young, W. R., "Ventilated and unventilated models of the wind-driven circulation," *J. Phys. Oceanogr.* **13,** 2020–2037 (1983).

Rhines, P. B., "The dynamics of unsteady currents," in *The Sea*, Vol. 6, E. D. Goldberg, I. N. McCabe, J. J. O'Brien and J. H. Steele, ed., Wiley, New York (1977).

Rhines, P. B. and Holland, W. R., "A theoretical discussion of eddy-driven mean flows," *Dynam. Atmos. Oceans* **3,** 289–325 (1979).

Rhines, P. B. and Young, W. R., "Potential vorticity homogenization in planetary gyres," *J. Fluid Mech.* **122,** 347–367 (1982a).

Rhines, P. B. and Young, W. R., "A theory of wind-driven circulation I. Mid-ocean gyres," *J. Mar. Res.* **40 Supplement,** 559–596 (1982b).

Rhines, P. B., "Gyration," *Ocean Modelling* **49,** Unpublished document (1983).

Rhines, P. B. and Young, W. R., "How rapidly is passive scalar mixed within closed streamlines?," *J. Fluid Mech.* **133,** 133–145 (1983).

Roache, P. J., *Computational Fluid Dynamics*, Hermosa Publishers, Albuquerque, New Mexico (1971).

Stommel, H. M., "A survey of ocean current theory," *Deep Sea Res.* **4,** 149–184 (1957).

Taylor, G. I., "Diffusion by continuous movements," *Proc. Lond. Math. Soc.* **20,** 196–212 (1921).

Taylor, G. I., "Dispersion of soluble matter in solvent flowing slowly through a tube," *Proc. R. Soc. Lond. A* **219,** 186–203 (1953).

Veronis, G. and Stommel, H. M., "The action of variable windstress on a stratified ocean," *J. Mar. Res.* **15,** 43–75 (1956).

Weiss, N., "The expulsion of magnetic flux by eddies," *Proc. R. Soc. Lond. A* **293,** 310–328 (1981).

Welander, P., "Effects of planetary topography on the deep-sea circulation," *Deep Sea Res.* **16 Supplement,** 369–392 (1969).

Young, W. R., "The vertical structure of the wind-driven circulation," *Ph.D. Dissertation*, WHOI/MIT Joint program in Oceanography (1981).

Young, W. R. and Rhines, P. B., "A theory of the wind-driven circulation. II. Circulation models and western boundary layers," *J. Mar. Res.* **40** (1982).

Young, W. R., "The role of western boundary layers in gyre-scale oceanic mixing," *J. Phys. Oceanogr*, In press (1983).